Accepted Manuscript

Periostin differentially induces proliferation, contraction and apoptosis of primary Dupuytren's Disease and adjacent palmar fascia cells

Linda Vi, Lucy Feng, Rebecca D Zhu, Yan Wu, Latha Satish, Bing Siang Gan, David B O'Gorman

Periostin differentially induces proliferation, contraction and apoptosis of primary Dupuytren's Disease and adjacent palmar fascia cells

Linda Vi[1,2#], Lucy Feng[1,2#], Rebecca D Zhu[1,2], Yan Wu[1,2], Latha Satish[3], Bing Siang Gan[1,2,4,5,6], and David B O'Gorman[1,2,4,7]*

#these authors contributed equally to this research.

[1]Cell & Molecular Biology Laboratory, Hand & Upper Limb Centre,

[2]Lawson Health Research Institute, London, Ontario, Canada, [3]Center for Genomic Sciences,

Allegheny-Singer Research Institute, Allegheny General Hospital, Pittsburgh, PA, U.S.A.,

[4]Departments of Surgery, [5]Physiology and Pharmacology, [6]Medical Biophysics and

[7]Biochemistry, University of Western Ontario, London, Ontario, Canada.

* Corresponding author:

E-mail: David B. O'Gorman: dogorman@uwo.ca

* The Hand and Upper Limb Centre,

St. Joseph's Health Centre,

268 Grosvenor Street

London, Ontario, Canada N6A 4L6

Phone: 519-646-6000 Ext: 64397   FAX: 519-646-6049

E-Mail: dogorman@uwo.ca

Abstract

Dupuytren's Disease, (DD), is a fibroproliferative condition of the palmar fascia in the hand, typically resulting in permanent contracture of one or more fingers. This fibromatosis is similar to scarring and other fibroses in displaying excess collagen secretion and contractile myofibroblast differentiation. In this report we expand on previous data demonstrating that *POSTN* mRNA, which encodes the extra-cellular matrix protein periostin, is up-regulated in Dupuytren's disease cord tissue relative to phenotypically normal palmar fascia. We demonstrate that the protein product of *POSTN*, periostin, is abundant in Dupuytren's disease cord tissue while little or no periostin immunoreactivity is evident in patient-matched control tissues. The relevance of periostin up-regulation in DD was assessed in primary cultures of cells derived from diseased and phenotypically unaffected palmar fascia from the same patients. These cells were grown in type-1 collagen-enriched culture conditions with or without periostin addition to more closely replicate the *in vivo* environment. Periostin was found to differentially regulate the apoptosis, proliferation, α smooth muscle actin expression and stressed fibroblast populated collagen lattice contraction of these cell types. We hypothesize that periostin, secreted by disease cord myofibroblasts into the extra-cellular matrix, promotes the transition of resident fibroblasts in the palmar fascia toward a myofibroblast phenotype, thereby promoting disease progression.

2

Introduction

Dupuytren's Disease (DD) is characterised by the progressive development of a scar-like, collagen-rich cord within the palmar fascia of the hand that typically results in permanent finger contracture. While DD can occur in both sexes and at all ages [1, 2], this fibromatosis is most common in males older than 70 years of Northern European descent [3, 4] with a reported prevalence as high as 39% in within some sections of this population [2]. The condition is currently incurable and is most commonly treated by surgical resection of the disease cord. Surgical resection has the disadvantages of being painful, requiring prolonged post-operative rehabilitation and disease recurrence rates after surgery are high [5-9]. Faced with these challenges, it is not unknown for patients with a history of multiple recurrences and/or surgery associated complications to opt for amputation of the affected finger(s) [10]. A detailed understanding of the cell biology of this condition is required before alternative treatment options including non-surgical molecular therapies can be developed.

Previous studies by several groups have identified *POSTN* mRNA as a highly up-regulated gene transcript in DD nodule and cord tissue relative to phenotypically normal palmar fascia control tissue [11-13]. *POSTN* encodes the extra-cellular matrix protein Periostin, originally identified as a TGFβ-1-inducible protein in osteoblasts (Osteoblast-Specific Factor-2 [14]). Periostin is highly expressed during the earliest stages of bone fracture repair [15] and vascular injury [16] and periostin signaling induces the expression of molecules associated with cutaneous wound repair such as collagen and fibronectin [17, 18]. A role in cancer cell metastasis has also been suggested, as periostin is a recognize component of stromal reactions in a variety of tumor types [19-29]. While DD shares some characteristics with each of these repair and disease processes, the role(s) of periostin in this fibromatosis are yet to be determined.

3

In this report we expand on these previous reports by assessing tissue lysates and sections of DD cord by real time PCR and *in situ* hybridization studies respectively. Further, we demonstrate that the protein product of *POSTN*, periostin, is abundant in involutional DD cord tissue relative to adjacent phenotypically normal palmar fascia from the same patients by western immunoblotting and immunohistochemistry. We have assessed the effects of recombinant periostin on primary DD and PF cell proliferation, α smooth muscle actin induction, apoptosis and contractility by adding this molecule to a type-1 collagen-enriched environment designed to more closely replicate *in vivo* conditions. Finally, we have interpreted our findings to speculate on the roles periostin might play in promoting DD cell development, as well as its potential to promote transition of adjacent palmar fascia to a disease phenotype.

Methods

Clinical Specimens

Nine surgically resected Dupuytren's Disease (DD) cord samples and small samples of phenotypically normal palmar fascia tissue (PF) were collected from patients undergoing primary surgical resection of palmar DD in the operating rooms of St Joseph's Health Care (SJHC), London, ON. No samples derived from patients undergoing surgery for DD recurrence were utilized in this study. All subjects provided written informed consent under institutional review board approval and specimens were collected with the approval of the University of Western Ontario Research Ethics Board for Health Sciences Research involving Human Subjects (HSREB protocol # 08222E) and in conformation with the Code of Ethics of the World Medical Association (Declaration of Helsinki) for experiments involving humans.

Total RNA Extraction

Approximately 100 mg tissue samples were crushed into small fragments on aluminum foil over dry ice, snap-frozen in liquid Nitrogen and ground in a mortar and pestle in 1 ml of TRIzol reagent (Invitrogen, Burlington, ON). Samples were transferred to 1.5 ml microcentrifuge tubes and total RNA was isolated using the TRIzol procedure. This RNA was then further purified using the RNeasy Minikit (Qiagen, Mississauga, ON). Aliquots (3 μl) were screened using an Agilent 2100 Bioanalyzer (Agilent Technologies, Mississauga, ON) and only high quality RNA samples were submitted to London Regional Genomic Center (www.lrgc.ca) for Microarray analysis on the Human Genome U133 Plus 2.0 Array (Affymetrix, Santa Clara CA).

Microarray Expression Analysis

Microarrray experiments were performed to identify genes that are differentially expressed in DD-affected palmar fascia versus those derived from normal fascia. Analysis was performed by the London Regional Genomic Center (www.lrgc.ca) using the Human Genome U133 Plus 2.0 Array (Affymetrix, Santa Clara, CA). The data were analyzed using the Significance Analysis of Microarrays (SAM) software package (http://222-stat.stanford.edu/~tibs/SAM/) at Center for Genomic Science, Allegheny-Singer Research Institute (Pittsburgh, PA). In brief, SAM computes a score for each gene that measures the strength of transcript correlation with differential expression. A threshold value was chosen for this small sample number analysis to give a false positive rate of 10%.

Real Time PCR

Confirmatory Real Time PCR quantitation of *POSTN* mRNA expression was performed on

5

an ABI Prism 7700 (Applied Biosystems, Foster City, CA) using the comparative Ct method. In brief, TRIzol reagent and RNeasy® Mini Kits (Qiagen, Mississauga, ON) were used to isolate total RNA from additional surgically resected tissues. RNA quality was again determined on an Agilent 2100 Bioanalyzer and 10μg of high quality total RNA was reverse transcribed into cDNA first strand using the High-Capacity cDNA Archive Kit (Applied Biosystems) in accordance with the manufacturer's instructions. For validity, the comparative Ct method requires that the amplification efficiency of the target and endogenous control transcripts to be equivalent. To assess this, dilutions of cDNA first strand corresponding to 1000ng, 500ng , 100ng, 50ng, 10ng and 0ng were introduced into the PCR reactions. Coupled with the target gene, *POSTN*, endogenous control gene products were amplified by gene specific probe sets containing TaqMan® MGB probes labeled with 6-FAM™ (Applied Biosystems, *POSTN*, Hs00170815_m1, endogenous control *GAPDH* 4333764F). Triplicate reactions of each dilution were performed (50 μl samples) in a 96-well plate format using SDS instrumentation (Applied Biosystems) for 45 cycles. Target and endogenous control reaction were run in separate wells in triplicate at each concentration. To determine if the target and endogenous control gene products amplified with the same efficiency, the ΔC_T value ($C_{T\ target}$ /$C_{T\ endogenous\ control}$) was plotted against the log input cDNA to create a semi-log regression line. A "pass" value of <0.2 for the slope of ΔC_T vs. log input was used in this study.

Western immunoblotting

Surgically resected DD tissue and patient-matched adjacent normal fascia were snap-frozen in liquid nitrogen and protein extracts were prepared using a tissue biopulveriser and PhosphoSafe protein Extraction Buffer (VWR, Mississauga, ON). Cell lysates were prepared in PhosphoSafe

6

protein Extraction Buffer in accordance with the manufacturer's instruction. After centrifuging

the extract to remove insoluble material, equivalent protein quantities were determined by BCA

analysis, subjected to immunoblotting and probed with antibodies against periostin (Santa Cruz

Biotechnology, Santa Cruz CA), α smooth muscle actin (AbCam, Cambridge MA) and β Actin

(Labvision, Fremont, CA). Immunoblot analysis was carried out using standard procedures and

immunoreactivity was visualized using Enhanced Chemiluminescence (ECL).

Immunohistochemistry

Four surgically resected DD cord and four patient-matched, phenotypically normal palmar fascia

samples were fixed in 10% formalin prior to dehydration, paraffin embedding and microtome

sectioning. Paraffin-embedded specimens were sectioned (5 μm), dewaxed, rehydrated and

treated with a 3% hydrogen peroxide solution to quench endogenous peroxidase activity. Slides

were treated with serum-free blocking reagent (Background Sniper, Biocare Medical, Concord,

CA) for 10 min and rinsed in PBS prior to incubation with periostin polyclonal antibody (1:1500

dilution, AbCam, Cambridge MA) or rabbit IgG (Dakocytomation, Mississauga, ON) overnight

at 4°C. After a wash in PBS, the slides were incubated (30 min, 22°C) with a biotinylated

secondary anti-rabbit antibody (Vector labs, Burlington ON), washed briefly in PBS, and

incubated (30 min, 22°C) with avidin/biotin/HRP complex (Vector elite PK-6100, Vector Labs,

Burlington ON). Finally, the slides were washed with PBS, and incubated (1 min) in an

enhanced di-amino benzidine (Cardassian DAB;Biocare Medical, Concord, CA). Sections were

counterstained with methyl green (10 min), dehydrated, cleared, and mounted with Permount

(Fisher Scientific, Ottawa, ON.).

Plasmid vectors and In Situ Hybridization

A 391-bp fragment encoding the N-terminus of periostin was excised using *Bam*HI and *Eco*RI

digestion of a human *POSTN* cDNA (a kind gift from Dr. Xiao-Fan Wang, Duke University

Medical Center, Durham, North Carolina) [26]. This fragment was cloned into pBluescript SK

(Stratgene, La Jolla, CA). Sense and antisense probes were generated in the presence of ^{35}S with

T7 and T3 RNA polymerases from plasmid linearized with *Bam* HI and *Eco*RI, respectively.

The *in situ* hybridization protocol used in this study has been described previously [30, 31]. In

brief, paraffin sections (5 µm thickness) of Dupuytren's disease cord and adjacent,

phenotypically normal palmar fascia were deparaffinized, rehydrated and permeablilized with

Triton X-100 and proteinase-K. Following prehybridization with 1x hybridization buffer, tissue

sections were hybridized with either ^{35}S-labelled antisense riboprobes or matching sense control

probes overnight at 60°C. Excess probe was washed off and the tissue sections were treated with

RNAse A to cleave non-hybridized probe. Tissue sections then underwent washes in decreasing

salt concentration and increasing temperature to a final stringency of 0.1 x standard saline citrate

at 60°C. Following dehydration, slides were then coated with nuclear track emulsion (NTB

nuclear track emulsion;Eastman Kodak, Rochester, NY) and exposed at 4°C for 11 days. Slides

were developed in D19 developer (Kodak), fixed, and counterstained with hematoxylin and

eosin.

Primary cell culture

Primary cells were isolated from surgically resected tissues as previously described (Howard et

al., 2004). The cultures were maintained in α-MEM-medium supplemented with 10% fetal

bovine serum (FBS, Invitrogen Corporation, Carlsbad, CA) and 1% antibiotic-antimycotic

solution (Sigma-Aldrich, St Louis, MO). All patient-matched primary cell lines were used up and until a maximum of 6 passages, during which no changes in cell morphology attributable to serial passage were evident. Our laboratory maintains a repository of greater than 50 primary cell lines derived from patient-matched DD and PF tissues and a minimum of three and a maximum of 6 primary DD and patient-matched PF cell lines were utilized for every analysis reported in this manuscript.

For *in vitro* culture on collagen, collagen fibers were mechanically extracted from rat tail tendons, placed under UV light overnight and then incubated in sterile acetic acid, with mechanical stirring for 7 days at 4°C. Undissolved collagen fibers were removed by centrifugation at 10,000 x g at 4°C for two hours. Collagen concentration was determined using the Sircol Collagen Quantification assay (Biocolor Ltd., Carrickfergus, UK). For tissue culture, collagen monolayers were cast in 6-well tissue culture trays with each well containing 800 ul collagen and 200 ul of the neutralization solution (2 parts 0.34 N NaOH and 3 parts 10x Waymouth media) to a final concentration of 1.9 mg/ml. Following collagen polymerization, primary cells were added in media with FBS and 1% antibiotic-antimycotic solution at 37°C in 5% CO_2 as described in the text. After 72 hours, media was aspirated from each well and cells were treated with vehicle or recombinant periostin (#3548-F2, R&D systems, Minneapolis, MN) at 0.5 μg/ml and/or 2.0 μg/ml as detailed in the Cell proliferation, Apoptosis and Fibroblast Populated Lattice methods described below. This recombinant protein is derived from a full-length *POSTN* cDNA with addition of a 6-HIS tag attached to the C-terminus of the protein and migrates in SDS PAGE at 90-95kDa under reducing conditions as predicted by the cDNA sequence (technical support, R&D systems, Minneapolis, MN).

Cell proliferation assays

The WST-1 assay (Millipore/Chemicon, Billerica, MA) was adapted to measure the proliferation of cells grown in collagen culture. In brief, 1×10^4 cells were plated in α MEM/2% FBS onto a 96 well tray pre-coated with 2 µg/ml periostin or vehicle (Phosphate Buffered Saline/0.1% BSA) in 60 µl of type-1 collagen (1.9 mg/ml) and incubated at 37ºC for 1, 3 or 6 days. WST-1 reagent was added to the wells to allow cleavage of the tetrazolium salt to formazan by cellular mitochondrial dehydrogenases. Equal volumes of supernatant were then transferred to an additional 96 well tray and absorbance measurements were performed at 450 nm and 595 nm (reference wavelength). All experiments were performed on a minimum of 3 matched cell lines and performed in triplicate.

Apoptosis assays

The Cell Death Detection ELISA (Roche Applied Science, Laval,QC) was used to detect histone-associated DNA fragments from mono- and oligonucleosomes as a marker for apoptotic cells. In brief, 1.2×10^5 cells per well were plated into 6 well plates coated with 1.9 mg/ml of type-1 collagen in 1ml of 10%FBS in αMEM in 37C in 5% CO2. After 3 days the cells were washed and made serum free for 12 hours before treatment with 0.5 or 2 µg/mL of recombinant Pn or vehicle in MCDB /1%FBS. MCDB media was utilized for these experiments as it is designed to enhance the long-term survival of human fibroblast-like cells in low serum conditions. After 4 days of treatment, the cells were washed with PBS and 1mL of 0.25mg/ml Collagenase XI (Sigma-Aldrich, St Louis, MO) was added to each well to remove cells from collagen. The cells were collected by centrifugation (300x g for 5 min) and resuspended in serum free medium. The cells were then spun at 1500X g for 5min, the supernatant discarded

10

and the cell pellet was resuspended with 500ul of lysis buffer and incubated at room temperature for 30 minutes. The lysate was then spun at 20,000x g for 10 minutes and the supernatant, which consist of the cytoplasmic fraction, was assayed using the ELISA according to the manufacturer's instructions. All experiments were performed on a minimum of 3 matched cell lines and performed in triplicate.

Stressed Fibroblast Populated Collagen Lattice (sFPCL) contractility assays

Collagen contraction assays were carried out using DD and control PF primary cell cultures established from diseased and adjacent uninvolved fascia from the same patients based on Tomasek *et al* [32]. Primary cultures (passages 3–6) were grown as three-dimensional Fibroblast Populated Collagen Lattices. Collagen lattices were cast in 24-well tissue culture trays with each well containing 400 μl collagen (final collagen concentration of 1.9 mg/ml), 100 μl neutralization solution, 1 x 10^5 cells and 2 μg/ml Pn or vehicle. FPCLs were maintained in a αMEM supplemented with 2% FBS and 1% antibiotic-antimycotic solution at 37°C in 5% CO_2 for 3 days. During this time, the primary fibroblasts in three dimensional collagen cultures respond to stress within the polymerized lattice and differentiate towards a contractile myofibroblast phenotype [33]. After 3 days in culture, all sFPCLs were simultaneously released from the sides and bottoms of the wells using a glass rod, allowing the differentiated myofibroblasts to contract the lattice. Lattices floating in tissue culture medium were digitally scanned at set intervals and the areas of each lattice were determined using the freehand tool in ImageJ software. Sequential area calculations were then normalized to the area prior to release. All experiments were performed on a minimum of 3 matched cell lines and each assay was performed in triplicate.

Statistical Analyses

Statistical analysis was conducted using SPSS v. 16 and Microsoft Excel 2007 statistical software. Paired t-tests were conducted on periostin and vehicle treated DD or PF cells at each time interval for cell proliferation, contractility, and apoptosis. Results were deemed significant when $p < 0.05$.

Results

POSTN mRNA and periostin are abundant in DD cord relative to control palmar fascia

We performed a small scale Affymetrix microarray analysis on total RNA extracted from two DD cord samples and one DD nodule sample for comparison with two patient-matched phenotypically normal palmar fascia samples and one additional normal palmar fascia sample obtained during carpal tunnel release surgery. As shown in **Table 1,** fourteen gene transcripts were identified as differentially regulated in all three DD samples by subsequent analysis of the data using SAM. The delta value was 7.539548891 and the FDR of this pilot study was 0.10138546, indicating that one of the genes detected maybe represent a random occurrence. Despite the small sample size, our data were consistent with previous larger scale studies [11, 12] in identifying two *POSTN* mRNA transcripts (gene IDs AY140646 and D13665) as up-regulated in DD tissue relative to controls.

Rather than expand our microarray analysis, we opted to confirm the changes in *POSTN* mRNA expression in additional surgical samples using real time PCR. *POSTN* mRNA levels were found to be highly variable across different sections of each DD cord, potentially reflecting the non-homogeneity of these surgically-resected tissues. Despite this within-sample variability,

12

mean *POSTN* mRNA levels were confirmed as significantly increased (p < 0.05) in all the surgically resected DD cord tissue samples relative to control samples (**Fig.1**).

To identify the cellular source(s) of *POSTN* mRNA in DD cord tissue, *in situ* hybridization studies were performed utilizing a *POSTN* cDNA on three additional DD cord and PF samples. As shown in **Fig.2 (A and B)**, hybridization with the antisense *POSTN* mRNA probe resulted in intense signal in densely cellular sections of the cord, where the most abundant cell type displayed a fibroblastic morphology, consistent with previous reports [32, 34-36]. Adjacent structures incorporated into the fibrotic cord, (such as the eccrine sweat duct shown in Fig 2, arrow), displayed relatively low levels of antisense *POSTN* mRNA probe hybridization. In contrast to signal evident in DD cord tissue, antisense *POSTN* mRNA probe signal was uniformly low in the less cellular, patient-matched, phenotypically normal palmar fascia (**Fig.2, B and C**). The sense *POSTN* mRNA probe exhibited uniform, low level background signal in all sections of the cord tissue, demonstrating the specificity of the antisense *POSTN* mRNA probe (**Fig.2, D and E**).

To determine if increased level of *POSTN* mRNA in DD tissue correlated with increased periostin levels, additional DD cord, nodular tissue and patient-matched, uninvolved palmar fascia samples were lysed and immunoblotted with periostin antibody. As shown in the representative immunoblot in **Fig.3A**, a major band with mobility of approximately 90kDa, corresponding to the predicted molecular weight of periostin (91.7 kDa), was evident in the DD cord tissue and nodule lysates assessed while little or no immunoreactivity was detected in patient-matched, uninvolved palmar fascia. Additional, less intense bands at lower molecular weights were evident in a subset of DD cord tissue samples, potentially representing degraded periostin. While periostin levels assessed by western immunoblotting were noted to vary

between patient-matched residual cord and nodule samples in a few instances (an example is

shown in **Fig. 3Ac**), the majority of densely cellular DD cord samples displayed readily

detectable levels of periostin. Immunohistochemistry revealed strong immunoreactivity

throughout cellular DD cord tissue while relatively little periostin immunoreactivity was evident

in patient-matched phenotypically normal palmar fascia (**Fig.3B, a and b**). Replacement of the

primary periostin antibody with IgG and subsequent addition of biotinylated secondary anti-

rabbit antibody followed by DAB addition confirmed the specificity of the primary antibody

interactions in these sections (data not shown).

Correlation of in vivo and in vitro periostin levels for primary cell culture

To determine appropriate levels of exogenous periostin treatment to approximate *in vivo*

conditions, 12μg of total protein extract from DD cord samples were compared to 0.25, 0.5, 1.0

and 2.0μg of recombinant full length periostin (R&D systems, Minneapolis, MN) by western

immunoblotting with periostin antibody. As shown in **Fig.4**, the recombinant periostin migrated

as two major bands at approximately 90 and 95 kDa (resulting from variable glycosylation

during production, R&D systems product information) as well as minor bands below 85 kDa,

potentially representing a mixture of periostin degradation products and low level cross-

reactivity with the vehicle carrier protein (0.1% BSA). The 90kDa species corresponded with

the periostin forms evident in DD cord at approximately 88-90kDa. Based on the intensity of the

most abundant molecular weight form of periostin in the DD cord samples, we estimated that

these samples contained between 0.5 and 2μg of periostin, or a range of 0.05 to 0.2μg of

periostin/μg of total protein. Based on this estimate, and $1x\ 10^5$ DD or PF cells routinely

yielding at least10μg of total protein in our hands, the data was extrapolated to conclude that a

treatment range of 0.5 to 2.0μg/ml of recombinant periostin to 1×10^5 cells in culture would

approximate *in vivo* levels. This range correlated with a previous report using 0.1μg/ml to 5μg/

ml periostin to assess apoptosis in cultures of pancreatic cancer cells [37].

Effects of periostin on apoptosis of DD and PF cells in collagen culture

To determine if exogenous periostin could modify the baseline apoptosis of DD or PF cells in

culture, three primary DD and three patient-matched PF cell lines were cultured for 4 days in 1%

FBS in MCDB media, designed to enhance long-term survival of human fibroblast-like cells in

low serum conditions, in the presence of vehicle, 0.5 and 2.0μg of recombinant periostin. The

cultures were then assessed for the presence of apoptotic cells using a Cell Death Detection

ELISA. As shown in **Fig.5**, cultures of DD cells treated with vehicle alone (Phosphate Buffered

Saline/0.1% BSA) contained significantly more cells undergoing apoptosis than cultures of PF

cells under identical culture conditions ($p < 0.05$). The addition of exogenous recombinant

periostin at 0.5 or 2 μg/mL to PF cell cultures resulted in a dose-dependent increase in apoptosis

relative to vehicle treated cells (both doses, $p < 0.05$). While a trend toward decreased apoptosis

was evident in all three DD cell lines treated with periostin, this effect varied between patients

and the mean values did not reach statistical significance at any of the concentrations tested

relative to vehicle treated cells.

Effects of periostin on proliferation of DD and PF cells in collagen culture

To determine if periostin affected the proliferative phenotype of DD or PF cells, cultures were

assessed using the WST-1 assay with vehicle or 2.0 μg/ml of recombinant periostin incorporated

in type-1 collagen over 6 days in α MEM with 2% FBS. As shown in **Fig.6**, periostin had no

15

significant effect on the basal proliferation rate of DD cells. In contrast, patient-matched PF

cells exhibited a consistent increase in cellular proliferation in all patient lines tested with

statistical significance being achieved by 6 days post treatment ($p < 0.05$).

Effects of periostin on contraction and α smooth muscle actin levels of DD and PF cells in

collagen culture

As DD is a contractile fibrosis characterized by myofibroblast abundance, we utilized stressed

Fibroblast Populated Collagen Lattice (sFPCL) assays to assess the effects of exogenous

periostin on DD and PF cell contractility. The degree of contraction of sFPCLs correlates with

the degree of myofibroblast differentiation in these cultures [33]. We have previously

demonstrated that DD cells display an increase in contractility in stressed FPCL assays compared

to patient matched PF cells [38]. As shown in **Fig.7A and B**, incorporation of periostin into the

collagen induced a statistically significant increase in DD cell contraction of collagen lattices

relative to vehicle treated DD cells at 12, 24 and 48 hours after release. Cell lysates derived from

FPCLs of DD and PF cells 48 hours after release were assessed by western immunoblotting for α

smooth muscle actin levels. As shown in **Fig.8**, periostin treatment of DD cells in FPCL culture

consistently induced a marked increase in α smooth muscle actin relative to vehicle treated DD

cells under identical conditions, consistent with previous studies correlating increased FPCL

contractility and induction of α smooth muscle actin [32]. These data contrasted with periostin-

treated PF cells in sFPCL culture at 48 hours after release, where α smooth muscle actin levels

were either unchanged, or occasionally modestly enhanced, by periostin treatment relative to

vehicle treated controls.

16

Discussion

The most widely accepted theory on the pathogenesis of DD is that resident fibroblasts in the palmar fascia are stimulated by as-yet unidentified factor(s) to undergo differentiation into a "nodule" of myofibroblasts, which in turn develop into a contractile disease "cord". The contractile forces that can, dependent on the site of the nodule within the palmar fascia, produce finger contracture are generated by these myofibroblasts. Much of this theory is based on the temporal correlation between the appearance of a densely cellular nodule containing randomly orientated spindle-shaped fibroblasts with increased α-smooth muscle actin expression (Luck's proliferative phase[39]) and the orientation of these cells along lines of tension corresponding to the onset of contraction (Luck's involution phase) [32, 35, 39-43]. It is apparent from many studies that nodular tissue is considered to be inherently more "biologically active" than the contracted cord tissue itself, which contains sections of densely collagenous and relatively acellular tissue [11, 44-46]. Despite this, primary cells derived from surgically resected nodular and cord tissue are very similar in appearance, in response to disease-associated cytokines such as TGFβ [44, 46] and in gene expression [13]. As surgically resected DD cords have been recognized for more than 50 years to contain both cell-dense and relatively acellular regions (Luck's "nodule-cord unit" [39]), we suggest that these data can be explained by primary culture selecting for a proliferative cellular pool within the cord that is common to both disease stages. These observations are consistent with our findings of abundant periostin in densely cellular sections of cord samples while residual cord samples from the same patient can display low levels of periostin (an example of which is shown in **Fig. 3Ac**). Based on these observations, we have taken advantage of the relative abundance of surgically resected cord samples containing

17

densely cellular tissue to derive our primary DD cells and used phenotypically normal palmar fascia tissue from the same patients as controls for our comparative analyses.

Originally identified as a TGFβ-1-inducible protein specific to mouse osteoblasts [14], periostin is now recognized as a ECM component of many collagen-rich connective tissues that are subjected to mechanical stress-tension [47]. Reports of *POSTN* mRNA up-regulation [11-13] and our data shown here demonstrating abundant periostin in a contractile fibrosis like DD, therefore, are not altogether unexpected. Periostin is a member of a subset of secreted ECM-associated molecules termed "matricellular" proteins [48-50] that modulate interactions with structural components of the ECM, such as collagens, and a variety of cell surface receptors, such as integrins, to regulate cellular differentiation in development [51] and connective tissue disease [52]. Based on these data and numerous studies demonstrating that the ECM can potently regulate cellular differentiation [53-57], where possible we incorporated our periostin treatments into the collagen substrate, rather than simply amending the tissue culture media, to more closely replicate *in vivo* conditions.

Periostin has been shown to promote collagen fibrillogenesis and alter the deposition of ECM proteins in other systems [58] and larger scale microarray studies have identified *COL1A1*mRNA, encoding the collagen α1 component of heterotrimeric and homotrimeric type-1 collagen [59], as up-regulated in DD cord [11, 12]. Excess collagen deposition and changes in ECM components are established hallmarks of DD [11, 60-62] and collagen in DD cords has been previously reported to feature increased levels of hydroxylysine and reducible cross-links, features also evident in scar tissue and indicative of abnormal deposition [63]. As variations in collagen type can also regulate fibroblast-mediated contractility *in vitro* [64], it is possible that periostin may play a role in collagen production, fibrillogenesis and cross-linking in DD. We are

currently addressing whether ECM-associated periostin can induces *COL1A1* mRNA expression in DD or PF cells and, if so, if this contribution to the ECM affects cellular contractility of these cells in sFPCLs. We are also interested in determining whether periostin specifically alters collagen cross-linking of these lattices and if this aspect contributes to the effects of periostin on FPCL contraction of DD cells.

We have demonstrated that collagen-bound periostin induces α-smooth muscle actin production and a significant increase in collagen lattice contraction by DD fibroblasts, consistent with this matricellular molecule promoting myofibroblast differentiation of these cells. While periostin-treated cultures of PF cells did not display a significant increase in contractility at any time point relative to vehicle treated cells, a consistent trend towards increased contractility was evident in the multiple experiments performed. We have also noted that α smooth muscle actin levels in PF cells were occasionally, but not consistently, up-regulated by periostin treatment in some cultures (data not shown). These data have led us to speculate that exposure to periostin in the ECM may induce PF cells to differentiate from a fibroblast phenotype toward a "proto-myofibroblast" phenotype, a transition phase prior to commitment to a differentiated myofibroblast phenotype, with inconsistently up-regulated α smooth muscle actin levels [65]. It will be interesting to test if a longer-term treatment of PF cells with ECM-associated periostin induces PF cells to take on a DD cell phenotype.

Myofibroblasts have been shown to utilize the PI3 kinase/Akt signaling pathway to avoid apoptosis in abnormal scarring [66-68] and periostin signaling has been shown to promote avoidance of apoptosis through this pathway [29, 37]. While there was a consistent trend towards a decrease in DD cells apoptosis with periostin treatment, this did not achieve statistical significance in our *in vitro* collagen culture conditions (DD cells treated with vehicle vs 0.5

µg/ml recombinant periostin, p = 0.075; PF cells treated with vehicle vs 2.0 µg/ml recombinant periostin, p = 0.065). Interestingly, multiple assessments of DD and PF cell lines cultured in type-1 collagen in the absence of periostin (treated with periostin vehicle, Phosphate Buffered Saline/0.1% BSA) revealed that DD cells consistently display a higher level of baseline apoptosis (p < 0.05) than their patient-matched PF controls. We speculate that these data reflect the sensitivity of DD myofibroblasts to the relatively low stress-tension of a collagen substrate relative to tissue culture plastic [69], further emphasizing the importance of modeling fibroproliferative diseases in culture systems that mimic the *in vivo* disease environment [70]. As previously discussed, it is possible that that longer term exposure to periostin may be required to detect any significant effects on DD cell apoptosis *in vitro*. As periostin up-regulation is associated with connective tissues with altered mechanical stress-tension [47], it will be interesting to determine whether the combination of mechanical tension and periostin in a collagenous environment will affect DD cell avoidance of apoptosis.

Our observations of significant increases in both proliferation and apoptosis in primary PF cells, cultured on collagen-coated dishes with exogenous periostin, are intriguing. We speculate that simultaneous periostin-induced proliferation and apoptosis of PF cells may be a component of their transition to a myofibroblast-like phenotype, although whether this implies a selection process for a subset of PF cells is currently unclear. Both DD and PF cells exhibit a basal rate of proliferation in our collagen-based two-dimensional cultures, unlike sFPCL cultures [38], possibly reflecting data indicating that sFPCL culture induces myofibroblast differentiation [43] and that terminally differentiated myofibroblasts do not proliferate [71]. Periostin was found to have no discernable effect on the basal proliferation rate of DD cells while inducing a significant increase in proliferation of PF cells. The induction of fibroblast proliferation followed by

differentiation into contractile fibroblasts is a normal component of the proliferative phase of cutaneous wound repair [72] and we speculate that one role of periostin may be to induce PF cells to initially proliferate and then eventually differentiate towards a proto-myofibroblast phenotype [65] with contractile bundles composed of cytoplasmic actins [73]. In contrast, primary DD cells in culture may already be in this proto-myofibroblast state, explaining why periostin treatment readily induced their differentiation to α smooth muscle actin expressing myofibroblasts. It is currently unclear whether the primary cells derived from DD cord tissue represent de-differentiated myofibroblasts or selection of a resident sub-population of proto-myofibroblasts in these tissues. Irrespective, it is clear from the induction of α smooth muscle actin and enhanced contractility reported here that periostin consistently induced these cells to assume a highly contractile, myofibroblast phenotype.

Clinically, full-thickness skin grafts (in which the dermis is included) have been shown to attenuate recurrence of DD in some studies [7, 74-76], implying that local environment of the DD cord left behind after resection may contain factors that promote disease recurrence. Our *in vitro* data suggest that PF fibroblasts, derived from the palmar fascia immediately adjacent to DD cord, are sensitive to periostin–induced proliferation. These data lead us to speculate that periostin secreted by DD cells into the surrounding ECM may potentially contaminate the adjacent fascia remaining after resection of the cord, promoting proliferation (and possibly, eventual myofibroblast differentiation) of the resident PF cells. Studies focused on long-term exposure of PF cells to periostin in *in vitro* culture systems that mimic the *in vivo* disease environment may shed light on this speculation.

Conclusion

Periostin is up-regulated component of DD cord that induces α smooth muscle actin formation and contraction primary DD cells. In addition, periostin was found to induce both PF cell proliferation and apoptosis. Further studies will be focused on elucidating the specific signaling pathways stimulated by periostin in these cell types and to determine if this molecule has potential as a target for therapeutic intervention to prevent DD recurrence.

Acknowledgements

Figure 1. Real Time PCR analysis of *POSTN* mRNA levels in normal palmar fascia and DD cord tissues.

POSTN mRNA levels were assessed in phenotypically normal palmar fascia and DD cord samples. Matching samples of PF and DD cord are shown for patient #4 (#4*) as well as normal palmar fascia from patient #5 compared to DD cord samples from patients (#6, #7). Triplicate analyses of *POSTN* mRNA levels were normalized to *GAPDH* mRNA expression using the comparative Ct method. Relative expression units (means and 95% confidence interval) are shown. Despite the variability inherent to cord samples of varying cellularity, the mean *POSTN* mRNA levels in each of the three DD cord samples were significantly increased relative to the phenotypically normal palmar fascia samples tested ($p < 0.05$).

Figure 2. *In situ* hybridization studies of POSTN mRNA expression in normal palmar fascia and DD cord tissues.

In situ hybridization studies performed using S^{35} labeled sense and antisense transcripts derived from a 391-bp fragment from the 5' end of a *POSTN* cDNA. Paraffin-embedded DD cord tissues (**A, B, E** and **F**) and palmar fascia tissue adjacent to the cord (**C** and **D**) were exposed to antisense *POSTN* mRNA probe (A, B, C and D) or sense POSTN mRNA probe control (**E** and **F**). Bright field images of Hematoxylin and Eosin stained tissues are shown in **A, C** and **E** while the same fields under dark field are shown in **B, D** and **F**. Silver grains deposited due to exposure to the S^{35} labeled transcripts are evident as uniform white specks under dark field. As shown, densely cellular DD cord tissue (**B**) exhibits intense antisense *POSTN* mRNA probe signal relative to low level signal in adjacent palmar fascia (**D**) or densely cellular DD cord tissue exposed to sense *POSTN* mRNA probe (**F**). All images are 400X.

Figure 3. Western immunoblotting and immunohistochemistry of periostin in normal palmar fascia and DD cord tissues.

A) Western immunoblots (a, b and c) for periostin in total protein lysates of surgically resected palmar fascia tissue (PF) and DD (DD) samples are shown. While each sample subjected to electrophoresis was adjusted to the same total protein concentration of the same, the cell: extracellular matrix ratio is different between densely cellular DD cord and phenotypically normal palmar fascia tissues. For this reason, intracellular β-actin levels were assessed to normalize the relative cellular contribution of each sample. As shown, periostin is readily detectable in total protein lysates of DD cord tissue but not patient matched palmar fascia while intracellular β-actin could be detected in both. An example of variable periostin immunoreactivity is shown (**c**, PF, DD nodule (DDn), DD cord (DDc)).

B) Immunohistochemistry of paraffin-embedded DD cord tissue (**a** and **c**) or adjacent, phenotypically normal palmar fascia (**b**) with periostin polyclonal antibody (**a** and **b**) or rabbit IgG (**c**). Periostin is evident as brown staining resulting from di-amino benzidine precipitation and all sections were counterstained with methyl green. As shown, abundant periostin is evident in densely cellular DD cord samples while relatively low-level immunoreactivity is evident in patient matched palmar fascia tissue.

Figure 4. Correlation of *in vivo* and *in vitro* periostin levels

To determine appropriate levels of exogenous periostin treatment to approximate *in vivo* conditions, total protein extracts (12μg) from four DD cords (DD) were compared to 0.25, 0.5, 1.0 and 2.0μg of recombinant periostin (R&D systems, Minneapolis, MN) by western

24

immunoblotting with periostin antibody (**A**). The relative sizes of recombinant periostin and endogenous periostin in DD cord are discussed in the text. The bands evident at 85-70kDa represent low-level cross reactivity with the serum albumin in the DD samples and BSA in the vehicle (Phosphate Buffered Saline/0.1% BSA). Based on the intensity of the most abundant molecular weight form of periostin in the DD cord samples, we estimated that the DD cord samples exhibited a range between 0.5μg and 2μg of periostin, or between 0.05μg to 0.2μg of periostin/μg of total protein. Based on this estimate and $1x\ 10^5$ DD or PF cells routinely yielding approximately 10μg of total protein in our hands, this data was extrapolated to conclude that a treatment range of 0.5 to 2.0μg/ml of recombinant periostin to 1×10^5 cells in culture would approximate *in vivo* levels.

Figure 5. Periostin effects on apoptosis of DD and PF cell in collagen culture.

The levels of apoptosis were assessed in cells growing on collagen substrate treated with vehicle or periostin in MCDB media using the Cell Death Detection ELISA . PF cells (while bars) and DD cells (black bars) were treated with vehicle (Phosphate Buffered Saline/0.1% BSA), 0.5 or 2.0 μg/ml recombinant periostin. PF and DD cells display a significant difference in baseline apoptosis with vehicle treatment (δ, $p < 0.05$). A significant increase in PF cell apoptosis is evident relative to vehicle treated cells for 0.5 μg/ml recombinant periostin, (*, $p < 0.05$) and 2.0 μg/ml recombinant periostin (*, $p < 0.01$). DD cells did not display a significant change in apoptosis relative to vehicle treatment with 0.5 μg/ml recombinant periostin ($p = 0.075$) or 2.0 μg/ml recombinant periostin ($p = 0.065$). Normalized absorbance units (mean ± Standard Error) are shown for three sets of patient-matched cell lines assessed three times in triplicate.

25

Figure 6. Periostin effects on DD and PF cell proliferation in collagen culture.

Proliferation assays were performed on DD and PF cells growing in collagen-enriched culture

containing recombinant periostin (2 μg/ml) or vehicle with using the WST-1 assay. As shown,

recombinant periostin induced a significant increase in PF cell proliferation compared to vehicle

treated cells (*, $p < 0.05$). DD cell proliferation was unaffected by addition of recombinant

periostin. Normalized absorbance units (mean ± Standard Error) are shown for six cell lines (3

patient-matched PF and DD) assessed three times in triplicate.

**Figure 7. Periostin effects on DD and PF cell stressed Fibroblast Populated Lattice Culture
(FPCL) contraction.**

Stressed FPCLs containing DD or PF cells and either recombinant periostin (2 μg/ml) or vehicle

were constructed as described in the methods. Lattices were photographed at various time

intervals after release (**A**) and the area of each lattice was determined using the freehand tool in

ImageJ software. Sequential area calculations were normalized to the area immediately after

release (0 hours post release) for three cell lines assessed three times in triplicate (**B**). The

horizontal axis denotes time (hours) after release and the vertical axis denotes the percentage

reduction in lattice area after release. As shown, cell-free collagen lattices (No cells) do not

contract significantly after release. Vehicle treated DD cells (DD-Veh) exhibit increased

contractility relative to vehicle treated PF cells (PF-Veh), consistent with our previous data [38].

2 μg/ml recombinant periostin induced a significant increase in DD cell contraction of the lattice

(DD-Pn) compared to vehicle treated cells (*, $p < 0.05$) at 12, 24 and 48 hrs after release,

indicative of increased myofibroblast contractility. No statistical difference in collagen

contraction was evident between periostin treated (PF-Pn) and vehicle treated PF cells ($p = 0.08$,

26

48 hours after release).

Figure 8. Periostin effects on α-smooth muscle actin induction by DD and PF cells in FPCL culture.

FPCLs containing DD or PF cells and either recombinant periostin (2 µg/ml, Pn) or vehicle (Veh) were lysed 48 hours after release and the lysates were subjected to western immunoblotting for α-smooth muscle actin. β actin levels were also assessed to confirm that equal amounts of cell-derived protein was loaded in each well. As shown, addition of 2 µg/ml periostin to the FPCL cultures of DD cells markedly induced α-smooth muscle actin accumulation. Recombinant periostin treatment of FPCL cultures containing PF cells did not consistently alter α-smooth muscle actin accumulation above cultures treated with vehicle. These immunoblots are representative of three PF and three DD cell lines assessed in triplicate.

References

1.	Urban, M., Feldberg, L., Janssen, A., and Elliot, D. (1996). Dupuytren's disease in children. *J Hand Surg [Br]* **21,** 112-6.
2.	Gudmundsson, K. G., Arngrimsson, R., Sigfusson, N., Bjornsson, A., and Jonsson, T. (2000). Epidemiology of Dupuytren's disease: clinical, serological, and social assessment. The Reykjavik Study. *J Clin Epidemiol* **53,** 291-6.
3.	Saboeiro, A. P., Porkorny, J. J., Shehadi, S. I., Virgo, K. S., and Johnson, F. E. (2000). Racial distribution of Dupuytren's disease in Department of Veterans Affairs patients. *Plast Reconstr Surg* **106,** 71-5.
4.	Saar, J. D., and Grothaus, P. C. (2000). Dupuytren's disease: an overview. *Plast Reconstr Surg* **106,** 125-34; quiz 135-6.
5.	Hakstian, R. (1974). "Late results of extensive fasciectomy," Grune and Stratton, New York.
6.	Norotte, G., Apoil, A., and Travers, V. (1988). A ten years follow-up of the results of surgery for Dupuytren's disease. A study of fifty-eight cases. *Ann Chir Main* **7,** 277-81.
7.	Jabaley, M. E. (1999). Surgical treatment of Dupuytren's disease. *Hand Clin* **15,** 109-26, vii.
8.	Mullins, P. A. (1999). Postsurgical rehabilitation of Dupuytren's disease. *Hand Clin* **15,** 167-74, viii.
9.	Gudmundsson, K. G., Arngrimsson, R., and Jonsson, T. (2001). Eighteen years follow-up study of the clinical manifestations and progression of Dupuytren's disease. *Scand J Rheumatol* **30,** 31-4.
10.	Kobus, K., Wojcicki, P., Dydymski, T., Wegrzyn, M., and Hamlawi, F. (2007). Evaluation of treatment results of patients with Dupuytren's contracture--our clinical experience. *Ortop Traumatol Rehabil* **9,** 134-40.
11.	Rehman, S., Salway, F., Stanley, J. K., Ollier, W. E., Day, P., and Bayat, A. (2008). Molecular phenotypic descriptors of Dupuytren's disease defined using informatics analysis of the transcriptome. *J Hand Surg [Am]* **33,** 359-72.
12.	Qian, A., Meals, R. A., Rajfer, J., and Gonzalez-Cadavid, N. F. (2004). Comparison of gene expression profiles between Peyronie's disease and Dupuytren's contracture. *Urology* **64,** 399-404.
13.	Shih, B., Wijeratne, D., Armstrong, D. J., Lindau, T., Day, P., and Bayat, A. (2009). Identification of biomarkers in Dupuytren's disease by comparative analysis of fibroblasts versus tissue biopsies in disease-specific phenotypes. *J Hand Surg [Am]* **34,** 124-36.
14.	Horiuchi, K., Amizuka, N., Takeshita, S., Takamatsu, H., Katsuura, M., Ozawa, H., Toyama, Y., Bonewald, L. F., and Kudo, A. (1999). Identification and characterization of a novel protein, periostin, with restricted expression to periosteum and periodontal ligament and increased expression by transforming growth factor beta. *J Bone Miner Res* **14,** 1239-49.
15.	Nakazawa, T., Nakajima, A., Seki, N., Okawa, A., Kato, M., Moriya, H., Amizuka, N., Einhorn, T. A., and Yamazaki, M. (2004). Gene expression of periostin in the early stage of fracture healing detected by cDNA microarray analysis. *J Orthop Res* **22,** 520-5.
16.	Lindner, V., Wang, Q., Conley, B. A., Friesel, R. E., and Vary, C. P. (2005). Vascular injury induces expression of periostin: implications for vascular cell differentiation and migration. *Arterioscler Thromb Vasc Biol* **25,** 77-83.

17. Erkan, M., Kleeff, J., Gorbachevski, A., Reiser, C., Mitkus, T., Esposito, I., Giese, T., Buchler, M. W., Giese, N. A., and Friess, H. (2007). Periostin Creates a Tumor-Supportive Microenvironment in the Pancreas by Sustaining Fibrogenic Stellate Cell Activity. *Gastroenterology*.

18. Butcher, J. T., Norris, R. A., Hoffman, S., Mjaatvedt, C. H., and Markwald, R. R. (2006). Periostin promotes atrioventricular mesenchyme matrix invasion and remodeling mediated by integrin signaling through Rho/PI 3-kinase. *Dev Biol*.

19. Forsti, A., Jin, Q., Altieri, A., Johansson, R., Wagner, K., Enquist, K., Grzybowska, E., Pamula, J., Pekala, W., Hallmans, G., Lenner, P., and Hemminki, K. (2006). Polymorphisms in the KDR and POSTN Genes: Association with Breast Cancer Susceptibility and Prognosis. *Breast Cancer Res Treat*.

20. Grigoriadis, A., Mackay, A., Reis-Filho, J. S., Steele, D., Iseli, C., Stevenson, B. J., Jongeneel, C. V., Valgeirsson, H., Fenwick, K., Iravani, M., Leao, M., Simpson, A. J., Strausberg, R. L., Jat, P. S., Ashworth, A., Neville, A. M., and O'Hare M, J. (2006). Establishment of the epithelial-specific transcriptome of normal and malignant human breast cells based on MPSS and array expression data. *Breast Cancer Res* **8,** R56.

21. Kudo, Y., Ogawa, I., Kitajima, S., Kitagawa, M., Kawai, H., Gaffney, P. M., Miyauchi, M., and Takata, T. (2006). Periostin promotes invasion and anchorage-independent growth in the metastatic process of head and neck cancer. *Cancer Res* **66,** 6928-35.

22. Tai, I. T., Dai, M., and Chen, L. B. (2005). Periostin induction in tumor cell line explants and inhibition of in vitro cell growth by anti-periostin antibodies. *Carcinogenesis* **26,** 908-15.

23. Siriwardena, B. S., Kudo, Y., Ogawa, I., Kitagawa, M., Kitajima, S., Hatano, H., Tilakaratne, W. M., Miyauchi, M., and Takata, T. (2006). Periostin is frequently overexpressed and enhances invasion and angiogenesis in oral cancer. *Br J Cancer* **95,** 1396-1403.

24. Sasaki, H., Dai, M., Auclair, D., Fukai, I., Kiriyama, M., Yamakawa, Y., Fujii, Y., and Chen, L. B. (2001). Serum level of the periostin, a homologue of an insect cell adhesion molecule, as a prognostic marker in nonsmall cell lung carcinomas. *Cancer* **92,** 843-8.

25. Sasaki, H., Dai, M., Auclair, D., Kaji, M., Fukai, I., Kiriyama, M., Yamakawa, Y., Fujii, Y., and Chen, L. B. (2001). Serum level of the periostin, a homologue of an insect cell adhesion molecule, in thymoma patients. *Cancer Lett* **172,** 37-42.

26. Sasaki, H., Lo, K. M., Chen, L. B., Auclair, D., Nakashima, Y., Moriyama, S., Fukai, I., Tam, C., Loda, M., and Fujii, Y. (2001). Expression of Periostin, homologous with an insect cell adhesion molecule, as a prognostic marker in non-small cell lung cancers. *Jpn J Cancer Res* **92,** 869-73.

27. Shao, R., Bao, S., Bai, X., Blanchette, C., Anderson, R. M., Dang, T., Gishizky, M. L., Marks, J. R., and Wang, X. F. (2004). Acquired expression of periostin by human breast cancers promotes tumor angiogenesis through up-regulation of vascular endothelial growth factor receptor 2 expression. *Mol Cell Biol* **24,** 3992-4003.

28. Gillan, L., Matei, D., Fishman, D. A., Gerbin, C. S., Karlan, B. Y., and Chang, D. D. (2002). Periostin secreted by epithelial ovarian carcinoma is a ligand for alpha(V)beta(3) and alpha(V)beta(5) integrins and promotes cell motility. *Cancer Res* **62,** 5358-64.

29. Bao, S., Ouyang, G., Bai, X., Huang, Z., Ma, C., Liu, M., Shao, R., Anderson, R. M., Rich, J. N., and Wang, X. F. (2004). Periostin potently promotes metastatic growth of colon cancer by augmenting cell survival via the Akt/PKB pathway. *Cancer Cell* **5,** 329-

39.
30.   Carter, A. M., Nygard, K., Mazzuca, D. M., and Han, V. K. (2006). The expression of insulin-like growth factor and insulin-like growth factor binding protein mRNAs in mouse placenta. *Placenta* **27,** 278-90.
31.   Han, V. K., Matsell, D. G., Delhanty, P. J., Hill, D. J., Shimasaki, S., and Nygard, K. (1996). IGF-binding protein mRNAs in the human fetus: tissue and cellular distribution of developmental expression. *Horm Res* **45,** 160-6.
32.   Tomasek, J., and Rayan, G. M. (1995). Correlation of alpha-smooth muscle actin expression and contraction in Dupuytren's disease fibroblasts. *J Hand Surg [Am]* **20,** 450-5.
33.   Dallon, J. C., and Ehrlich, H. P. (2008). A review of fibroblast-populated collagen lattices. *Wound Repair Regen* **16,** 472-9.
34.   Gabbiani, G., and Majno, G. (1972). Dupuytren's contracture: fibroblast contraction? An ultrastructural study. *Am J Pathol* **66,** 131-46.
35.   Tomasek, J. J., Schultz, R. J., Episalla, C. W., and Newman, S. A. (1986). The cytoskeleton and extracellular matrix of the Dupuytren's disease "myofibroblast": an immunofluorescence study of a nonmuscle cell type. *J Hand Surg [Am]* **11,** 365-71.
36.   Magro, G., Fraggetta, F., Travali, S., and Lanzafame, S. (1997). Immunohistochemical expression and distribution of alpha2beta1, alpha6beta1, alpha5beta1 integrins and their extracellular ligands, type IV collagen, laminin and fibronectin in palmar fibromatosis. *Gen Diagn Pathol* **143,** 203-8.
37.   Baril, P., Gangeswaran, R., Mahon, P. C., Caulee, K., Kocher, H. M., Harada, T., Zhu, M., Kalthoff, H., Crnogorac-Jurcevic, T., and Lemoine, N. R. (2006). Periostin promotes invasiveness and resistance of pancreatic cancer cells to hypoxia-induced cell death: role of the beta(4) integrin and the PI3k pathway. *Oncogene*.
38.   Tse, R., Howard, J., Wu, Y., and Gan, B. S. (2004). Enhanced Dupuytren's disease fibroblast populated collagen lattice contraction is independent of endogenous active TGF-beta2. *BMC Musculoskelet Disord* **5,** 41.
39.   Luck, J. V. (1959). Dupuytren's contracture; a new concept of the pathogenesis correlated with surgical management. *J Bone Joint Surg Am* **41-A,** 635-64.
40.   Hurst, L. C., Badalamente, M. A., and Makowski, J. (1986). The pathobiology of Dupuytren's contracture: effects of prostaglandins on myofibroblasts. *J Hand Surg [Am]* **11,** 18-23.
41.   Iwasaki, H., Muller, H., Stutte, H. J., and Brennscheidt, U. (1984). Palmar fibromatosis (Dupuytren's contracture). Ultrastructural and enzyme histochemical studies of 43 cases. *Virchows Arch A Pathol Anat Histopathol* **405,** 41-53.
42.   Rayan, G. M., Parizi, M., and Tomasek, J. J. (1996). Pharmacologic regulation of Dupuytren's fibroblast contraction in vitro. *J Hand Surg [Am]* **21,** 1065-70.
43.   Rayan, G. M., and Tomasek, J. J. (1994). Generation of contractile force by cultured Dupuytren's disease and normal palmar fibroblasts. *Tissue Cell* **26,** 747-56.
44.   Dave, S. A., Banducci, D. R., Graham, W. P., 3rd, Allison, G. M., and Ehrlich, H. P. (2001). Differences in alpha smooth muscle actin expression between fibroblasts derived from Dupuytren's nodules or cords. *Exp Mol Pathol* **71,** 147-55.
45.   Seyhan, H., Kopp, J., Schultze-Mosgau, S., and Horch, R. E. (2006). Increased metabolic activity of fibroblasts derived from cords compared with nodule fibroblasts sampling from patients with Dupuytren's contracture. *Plast Reconstr Surg* **117,** 1248-52.

46. Bisson, M. A., McGrouther, D. A., Mudera, V., and Grobbelaar, A. O. (2003). The different characteristics of Dupuytren's disease fibroblasts derived from either nodule or cord: expression of alpha-smooth muscle actin and the response to stimulation by TGF-beta1. *J Hand Surg [Br]* **28,** 351-6.

47. Norris, R. A., Damon, B., Mironov, V., Kasyanov, V., Ramamurthi, A., Moreno-Rodriguez, R., Trusk, T., Potts, J. D., Goodwin, R. L., Davis, J., Hoffman, S., Wen, X., Sugi, Y., Kern, C. B., Mjaatvedt, C. H., Turner, D. K., Oka, T., Conway, S. J., Molkentin, J. D., Forgacs, G., and Markwald, R. R. (2007). Periostin regulates collagen fibrillogenesis and the biomechanical properties of connective tissues. *J Cell Biochem*.

48. Bornstein, P. (1995). Diversity of function is inherent in matricellular proteins: an appraisal of thrombospondin 1. *J Cell Biol* **130,** 503-6.

49. Bornstein, P. (2000). Matricellular proteins: an overview. *Matrix Biol* **19,** 555-6.

50. Bornstein, P., and Sage, E. H. (2002). Matricellular proteins: extracellular modulators of cell function. *Curr Opin Cell Biol* **14,** 608-16.

51. Norris, R. A., Borg, T. K., Butcher, J. T., Baudino, T. A., Banerjee, I., and Markwald, R. R. (2008). Neonatal and adult cardiovascular pathophysiological remodeling and repair: developmental role of periostin. *Ann N Y Acad Sci* **1123,** 30-40.

52. Hamilton, D. W. (2008). Functional role of periostin in development and wound repair: implications for connective tissue disease. *J Cell Commun Signal*.

53. Boudreau, N. J., and Jones, P. L. (1999). Extracellular matrix and integrin signalling: the shape of things to come. *Biochem J* **339 (Pt 3),** 481-8.

54. Daley, W. P., Peters, S. B., and Larsen, M. (2008). Extracellular matrix dynamics in development and regenerative medicine. *J Cell Sci* **121,** 255-64.

55. Lock, J. G., Wehrle-Haller, B., and Stromblad, S. (2008). Cell-matrix adhesion complexes: master control machinery of cell migration. *Semin Cancer Biol* **18,** 65-76.

56. Lukashev, M. E., and Werb, Z. (1998). ECM signalling: orchestrating cell behaviour and misbehaviour. *Trends Cell Biol* **8,** 437-41.

57. Rosso, F., Giordano, A., Barbarisi, M., and Barbarisi, A. (2004). From cell-ECM interactions to tissue engineering. *J Cell Physiol* **199,** 174-80.

58. Snider, P., Hinton, R. B., Moreno-Rodriguez, R. A., Wang, J., Rogers, R., Lindsley, A., Li, F., Ingram, D. A., Menick, D., Field, L., Firulli, A. B., Molkentin, J. D., Markwald, R., and Conway, S. J. (2008). Periostin is required for maturation and extracellular matrix stabilization of noncardiomyocyte lineages of the heart. *Circ Res* **102,** 752-60.

59. Ottani, V., Martini, D., Franchi, M., Ruggeri, A., and Raspanti, M. (2002). Hierarchical structures in fibrillar collagens. *Micron* **33,** 587-96.

60. Bailey, A. J., Sims, T. J., Gabbiani, G., Bazin, S., and LeLous, M. (1977). Collagen of Dupuytren's disease. *Clin Sci Mol Med* **53,** 499-502.

61. Berndt, A., Kosmehl, H., Katenkamp, D., and Tauchmann, V. (1994). Appearance of the myofibroblastic phenotype in Dupuytren's disease is associated with a fibronectin, laminin, collagen type IV and tenascin extracellular matrix. *Pathobiology* **62,** 55-8.

62. Satish, L., Laframboise, W. A., O'Gorman, D. B., Johnson, S., Janto, B., Gan, B. S., Baratz, M. E., Hu, F. Z., Post, J. C., Ehrlich, G. D., and Kathju, S. (2008). Identification of differentially expressed genes in fibroblasts derived from patients with Dupuytren's Contracture. *BMC Med Genomics* **1,** 10.

63. Brickley-Parsons, D., Glimcher, M. J., Smith, R. J., Albin, R., and Adams, J. P. (1981). Biochemical changes in the collagen of the palmar fascia in patients with Dupuytren's

disease. *J Bone Joint Surg [Am]* **63,** 787-97.

64. Ehrlich, H. P. (1988). The modulation of contraction of fibroblast populated collagen lattices by types I, II, and III collagen. *Tissue Cell* **20,** 47-50.

65. Tomasek, J. J., Gabbiani, G., Hinz, B., Chaponnier, C., and Brown, R. A. (2002). Myofibroblasts and mechano-regulation of connective tissue remodelling. *Nat Rev Mol Cell Biol* **3,** 349-63.

66. Shi-Wen, X., Chen, Y., Denton, C. P., Eastwood, M., Renzoni, E. A., Bou-Gharios, G., Pearson, J. D., Dashwood, M., du Bois, R. M., Black, C. M., Leask, A., and Abraham, D. J. (2004). Endothelin-1 promotes myofibroblast induction through the ETA receptor via a rac/phosphoinositide 3-kinase/Akt-dependent pathway and is essential for the enhanced contractile phenotype of fibrotic fibroblasts. *Mol Biol Cell* **15,** 2707-19.

67. Wynes, M. W., Frankel, S. K., and Riches, D. W. (2004). IL-4-induced macrophage-derived IGF-I protects myofibroblasts from apoptosis following growth factor withdrawal. *J Leukoc Biol* **76,** 1019-27.

68. Horowitz, J. C., Rogers, D. S., Sharma, V., Vittal, R., White, E. S., Cui, Z., and Thannickal, V. J. (2007). Combinatorial activation of FAK and AKT by transforming growth factor-beta1 confers an anoikis-resistant phenotype to myofibroblasts. *Cell Signal* **19,** 761-71.

69. Hinz, B., Phan, S. H., Thannickal, V. J., Galli, A., Bochaton-Piallat, M. L., and Gabbiani, G. (2007). The myofibroblast: one function, multiple origins. *Am J Pathol* **170,** 1807-16.

70. Vi, L., Njarlangattil, A., Wu, Y., Gan, B. S., and O'Gorman, D. B. (2009). Type-1 collagen differentially alters beta-catenin accumulation in primary Dupuytren's Disease cord and adjacent palmar fascia cells. *BMC Musculoskelet Disord* **10,** 72.

71. Grotendorst, G. R., Rahmanie, H., and Duncan, M. R. (2004). Combinatorial signaling pathways determine fibroblast proliferation and myofibroblast differentiation. *Faseb J* **18,** 469-79.

72. Darby, I. A., and Hewitson, T. D. (2007). Fibroblast differentiation in wound healing and fibrosis. *Int Rev Cytol* **257,** 143-79.

73. Hinz, B. (2007). Formation and function of the myofibroblast during tissue repair. *J Invest Dermatol* **127,** 526-37.

74. Hall, P. N., Fitzgerald, A., Sterne, G. D., and Logan, A. M. (1997). Skin replacement in Dupuytren's disease. *J Hand Surg [Br]* **22,** 193-7.

75. Brotherston, T. M., Balakrishnan, C., Milner, R. H., and Brown, H. G. (1994). Long term follow-up of dermofasciectomy for Dupuytren's contracture. *Br J Plast Surg* **47,** 440-3.

76. Armstrong, J. R., Hurren, J. S., and Logan, A. M. (2000). Dermofasciectomy in the management of Dupuytren's disease. *J Bone Joint Surg Br* **82,** 90-4.

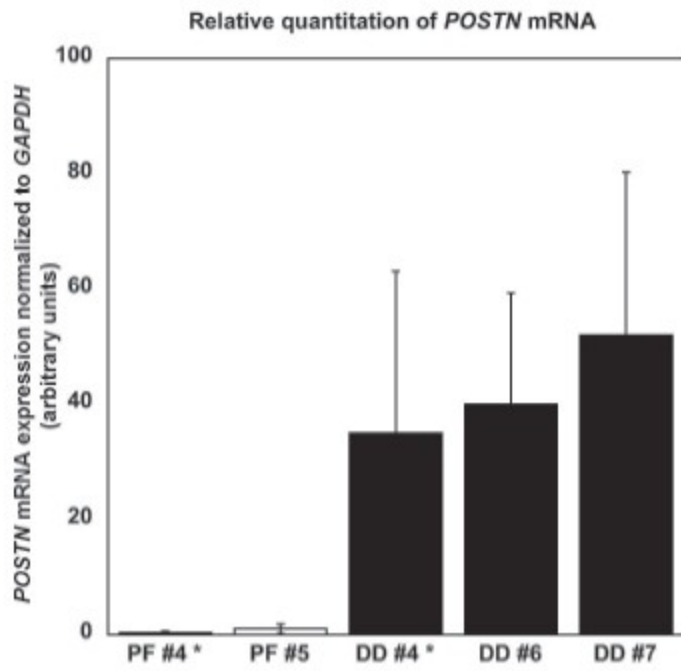**Table 1   A) SAM analysis of gene transcripts up-regulated in DD samples vs**

phenotypically unaffected palmar fascia

	Gene ID	Gene Name	Fold Change
1.	**AY140646**	**Homo sapiens extracellular matrix protein periostin-bm mRNA, complete cds**	**62.79**
2.	NM_025061	Homo sapiens hypothetical protein FLJ23420 (FLJ23420), mRNA	6.53
3.	**D13665**	**Homo sapiens osf-2 mRNA for osteoblast specific factor 2 (OSF-2p1), complete cds**	**7.92**
4.	AI917494	Homo sapiens cDNA clone IMAGE:2237989 3-, mRNA sequence	6.28
5.	AY007239	Homo sapiens monooxygenase X mRNA, complete cds	4.18
6.	AI214061	Homo sapiens cDNA clone IMAGE:1956787 3- similar to gb:X05276_cds1 Tropomyosin, fibroblast non muscle type (human); mRNA sequence	4.13
7.	AF362887	Homo sapiens tropomyosin 4-anaplastic lymphoma kinase fusion protein minor isoform mRNA	3.24

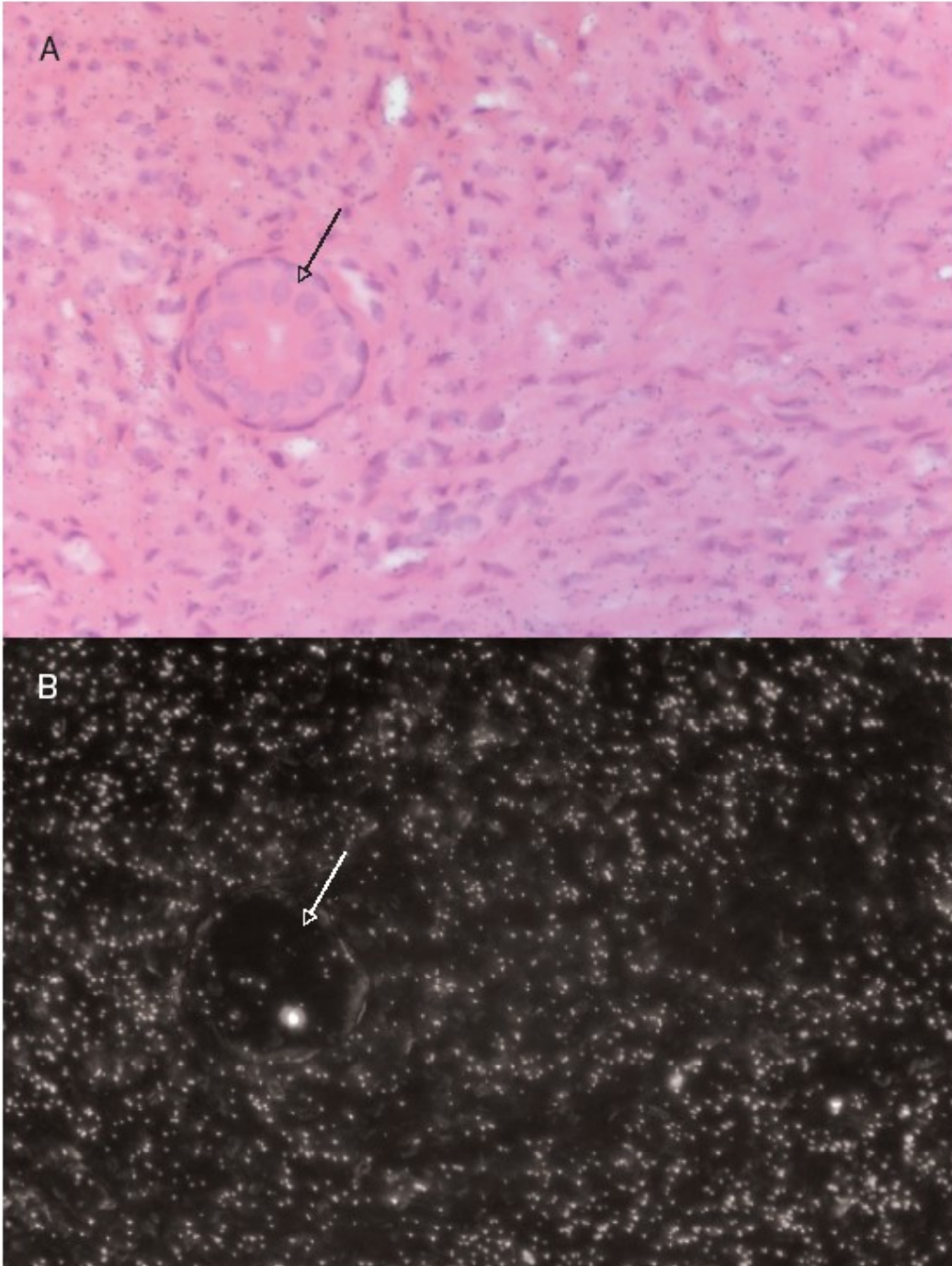**B) SAM analysis of gene transcripts down regulated in DD samples vs**
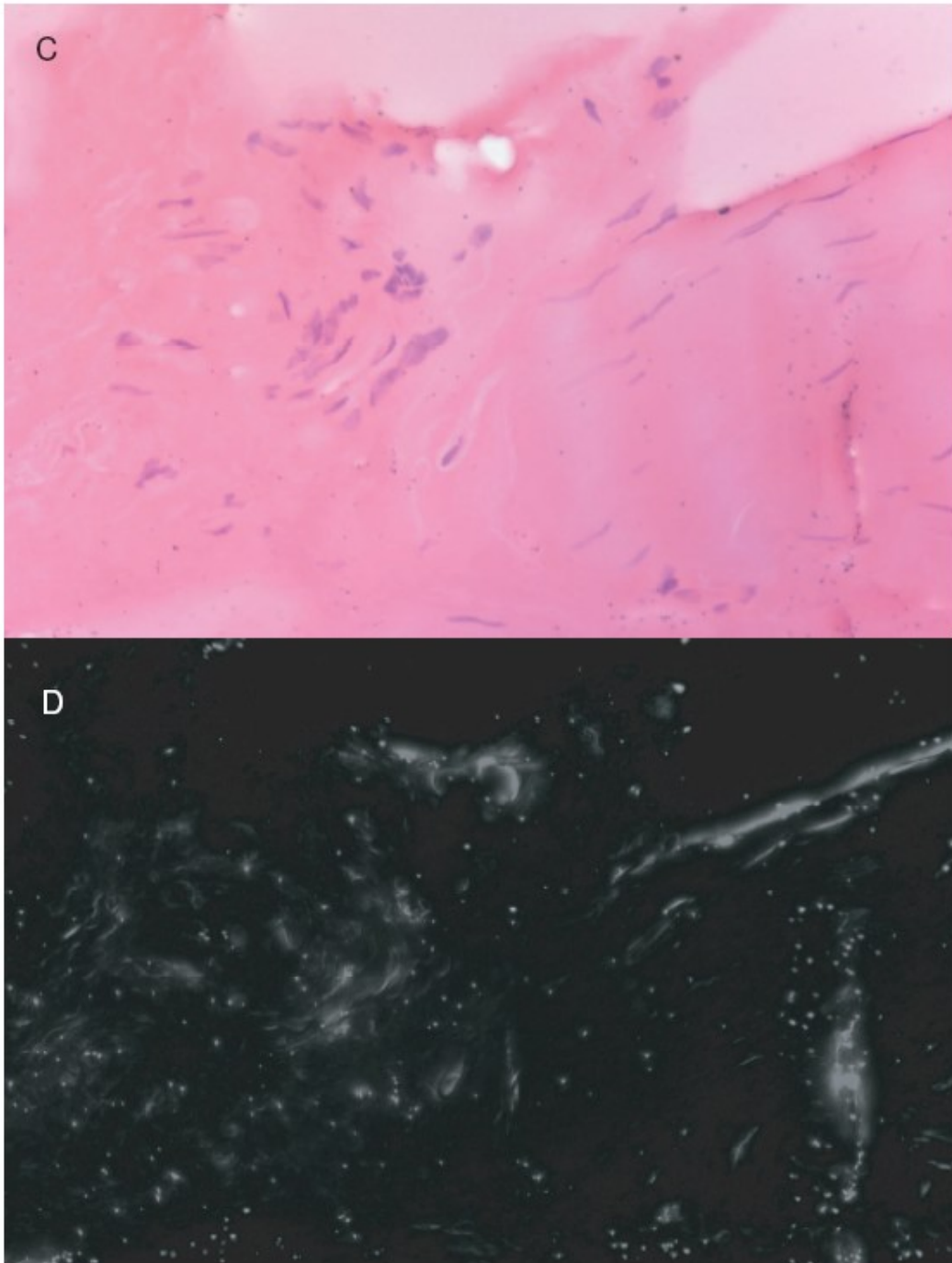
phenotypically unaffected palmar fascia

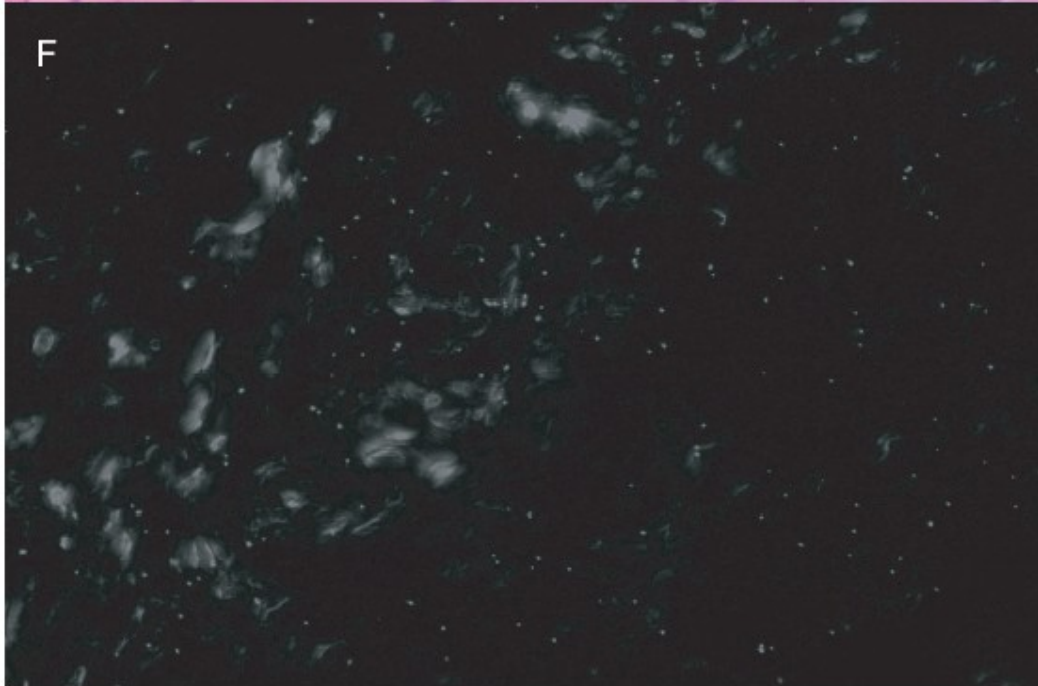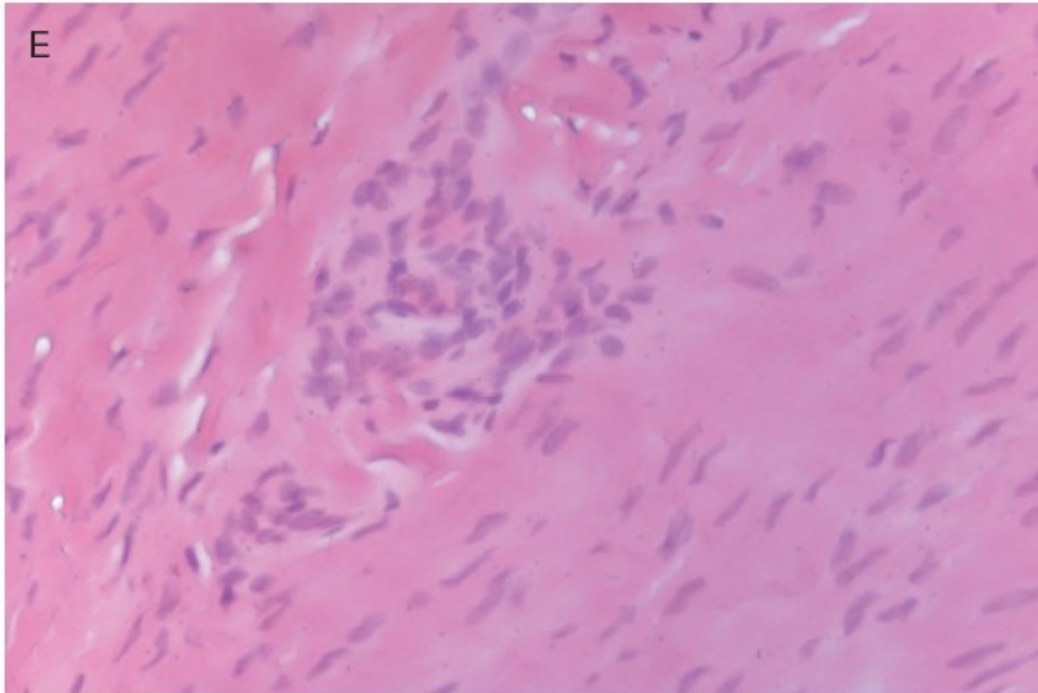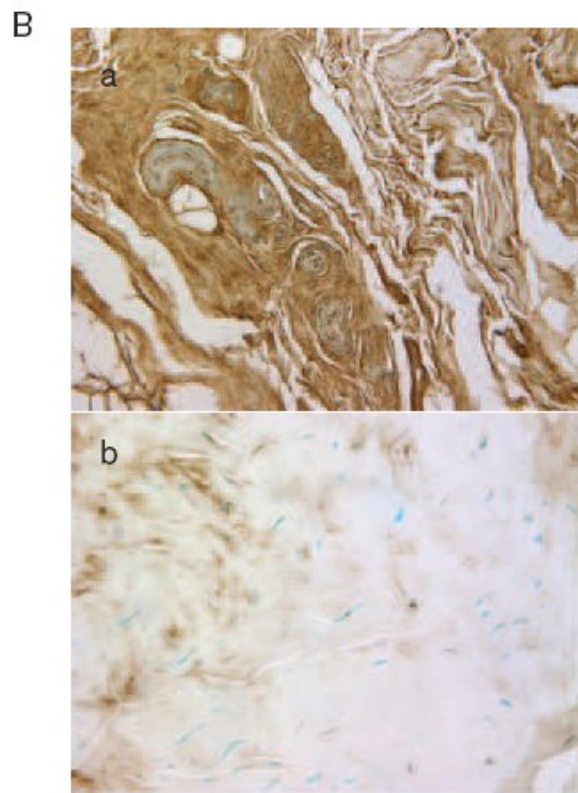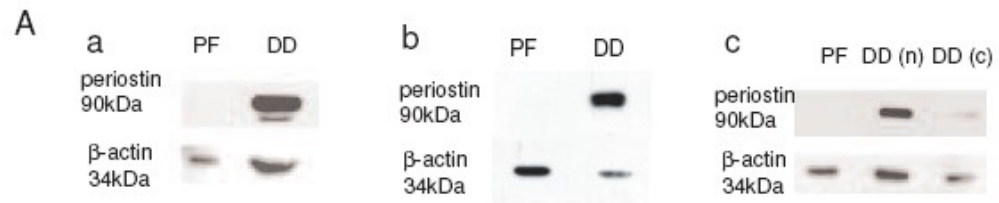|	Gene ID	Gene Name	Fold Change
1.	AI828075	wk31e04.x1 NCI_CGAP_Brn25 Homo sapiens cDNA clone IMAGE:2413950 3-, mRNA sequence	0.38
2.	AI078167	nuclear factor of kappa light polypeptide gene enhancer in B-cells inhibitor, alpha /FL	0.33
3.	Z83851	Human DNA sequence from clone CTA-989H11 on chromosome 22q13.1-13.2 Contains three novel genes, the 5' end of a novel gene and four CpG islands, complete sequence	0.28
4.	AU153267	AU153267 NT2RP3 Homo sapiens cDNA clone NT2RP3002763 3-, mRNA sequence	0.25
5.	AA224115	gi:1844674 /DB_XREF=zr14c05.r1 /Clone=IMAGE:648776 /FEA=EST /CNT=5 /TID=Hs.193444.0 /Tier=ConsEnd /STK=0 /UG=Hs.193444 /UG	0.21
6.	AF288406	Homo sapiens G protein interaction factor 2-like mRNA sequence /DEF=Homo sapiens G protein interaction factor 2-like mRNA sequence	0.17
7.	AL080077	Homo sapiens mRNA; cDNA DKFZp564C0962 (from clone DKFZp564C0962) /DEF=Homo sapiens mRNA; cDNA DKFZp564C0962 (from clone DKFZp564C0962)	0.15

Relative quantitation of *POSTN* mRNA

WST-1 proliferation assay

A

PF — DD

Pn — Veh — Pn — Veh

2 hrs

12 hrs

24 hrs

B

Stressed FPCL contraction assay

No cells
PF-Veh
PF-Pn
DD-Veh
DD-Pn

hours post release

Percent reduction in lattice area

PF   DD

Veh   Pn   Veh   Pn

α Smooth
Muscle Actin
43 kDa

β Actin
43 kDa